Available online at www.sciencedirect.com

ScienceDirect

Ceramics International 40 (2014) 5039–5042

CERAMICS INTERNATIONAL

www.elsevier.com/locate/ceramint

Short communication

# Co-synthesis of ZnO/$SnO_2$ mixed nanowires via a single-step carbothermal reduction method

T. Tharsika[a], A.S.M.A Haseeb[a,*], S.A. Akbar[b], M.F.M. Sabri[a]

[a]Department of Mechanical Engineering, Faculty of Engineering, University of Malaya, 50603 Kuala Lumpur, Malaysia
[b]Department of Materials Science and Engineering, Ohio State University, 2041 College Road, Columbus, OH 43210, USA

Received 2 August 2013; received in revised form 31 August 2013; accepted 31 August 2013
Available online 7 September 2013

**Abstract**

ZnO/$SnO_2$ mixed nanowires are fabricated by a single-step in-situ carbothermal reduction of mixed ZnO and $SnO_2$ powders with activated carbon under atmospheric pressure on a gold (Au) coated alumina substrate. Morphology and structural properties of the mixed nanowires are studied by field emission scanning electron microscopy (FESEM), X-ray diffraction (XRD) and transmission electron microscopy (TEM). FESEM investigation reveals the presence of uniform straight nanowires and branched hierarchical nanowires. The mixed nanowires have a diameter of about 15–80 nm and length ranging from two to several tens of micrometers, and thus having an aspect ratio above 1000. X-ray diffraction patterns show the crystalline nature of the ZnO/$SnO_2$ mixed nanowires. Elemental mapping in a TEM suggests that the ZnO and $SnO_2$ phases are mixed uniformly in the nanowire.
© 2013 Elsevier Ltd and Techna Group S.r.l. All rights reserved.

*Keywords:* B. Electron microscopy; ZnO/$SnO_2$ mixed nanowire; Hierarchical nanostructure; Carbothermal reduction

## 1. Introduction

One-dimensional metal oxide semiconductor nanostructures have attracted noteworthy attention from researchers because of their electrical, chemical and optical properties [1,2] which lead to potential applications in catalysis [3], chemical and biological sensors [3,4], photodetectors [5], and lithium-ion batteries [6]. Mixed oxide nanowires with hierarchical and core–shell structures have received considerable attention as they can offer improved electrical properties, such as carrier concentration and conductivity, suitable for photovoltaic (PV) energy conversion and chemical sensing [7]. Hybrid one-dimensional nanostructures of mixed metal oxide semiconductors, such as $SnO_2/W_{18}O_{49}$ [7], ZnO/$SnO_2$ [8–11], $CeO_2/TiO_2$ [12], $TiO_2$/ZnO [13], α-$Fe_2O_3/SnO_2$ [14], and α-$Fe_2O_3$/ZnO [15] have been synthesized by a variety of methods and they have shown better photovoltaic and chemical sensing properties compared to single oxide 1D structures. Among these oxides, ZnO ($E_g \sim 3.37$ eV) and $SnO_2$ ($E_g \sim 3.6$ eV) are wide band gap and key functional materials, which have been widely studied [16–19]. Recently, ZnO/$SnO_2$ mixed nanowires have been synthesized by a number of techniques, such as, vapor phase transport processes [20,21], the two-step carbon assisted thermal evaporation method [8,22], electrospinning [9,10], chemical vapor transport and condensation [23], and the hydrothermal method [20,24]. Until now, most of the ZnO/$SnO_2$ mixed nanostructures have been reported to be produced by a two-step method at low pressure, where each oxide is synthesized by the carbothermal reduction method sequentially. For example, Hwang et al. [8] synthesized ZnO/$SnO_2$ core–shell nanowires via a two-step carbothermal reduction method with pressure inside the system maintained around $10^{-2}$ Torr, while Lan et al. [22] produced hierarchical nanostructures at a pressure of 1 Pa.

This paper reports ZnO/$SnO_2$ nanowires synthesized by a single-step carbothermal reduction, which is a relatively facile method compared to the above mentioned techniques. All these methods except electrospinning and hydrothermal, are either governed by the vapour–solid (VS) mechanism or the catalyst assisted vapour-liquid-solid (VLS) mechanism. The work reported here employs the catalyst assisted VLS

*Corresponding author. Tel.: +603 7967 4598; fax: +603 7967 4448.
*E-mail addresses:* tharsika@siswa.um.edu.my (T. Tharsika), haseeb@um.edu.my (A.S.M. Haseeb), akbar.1@osu.edu (S.A. Akbar), faizul@um.edu.my (M.F.M. Sabri).

0272-8842/$ - see front matter © 2013 Elsevier Ltd and Techna Group S.r.l. All rights reserved.
http://dx.doi.org/10.1016/j.ceramint.2013.08.142

mechanism. In this process, metal nanoparticles or nanoclusters are used as nucleation seeds. These nucleation seeds determine the growth direction, interfacial energy and diameter of the 1-D metal oxide nanowires [25]. In this facile method, the morphology and properties of nanowires are generally controlled by growth parameters such as temperature, thickness of catalyst layer, rate of carrier gas flow, and distance between the source and the substrate [26]. Morphology and structural characterizations of the fabricated crystalline ZnO/$SnO_2$ mixed nanowires are presented and discussed.

## 2. Experimental procedure

The synthesis of ZnO/$SnO_2$ mixed nanowires in this work involved a carbothermal reduction process. Here activated carbon powder acts as a reducing agent for the metal oxide powders. Commercial ZnO (350 nm, 99% purity, Sigma-Aldrich), $SnO_2$ (~325 mesh, 99.9% trace metals basis, Sigma-Aldrich) and activated carbon (R&M Chemicals, UK) powders with a molar ratio of 9:1:10 were ground together by ball milling for 8 h to get a homogeneous mixture of nanoparticles with an average particle size of 150 nm. A thin Au layer of 40 Å thickness was deposited on an alumina substrate by a sputter coater. A quartz boat loaded with milled powder mixture was placed in the center of a horizontal tube furnace (Lindberg Blue M: TF55035COMA1). The substrate was located at 9.5 cm away from the source powder. Then Ar (purity 99.99%) was introduced as a carrier gas with a constant flow rate of 25 sccm throughout the process. The temperature of the furnace was increased from room temperature to 900 °C at a rate of 30 °C $min^{-1}$. This temperature was maintained for a growth time of 2 h and subsequently cooled down to room temperature. A light gray layer was observed on the alumina substrate after being cooled down to room temperature. The control experiments were conducted with two samples: (1) with activated carbon and no Au layer and (2) with Au layer and no activated carbon.

The as-prepared samples were collected for phase identification by X-ray diffraction (XRD) using a PANalytical Empyrean utilizing CuKα radiation (1.54059 Å). The morphology of the synthesized nanowires was determined by a field emission scanning electron microscopy (FESEM, Auriga Zeiss Ultra-60). The morphological features and elemental distribution were characterized by a transmission electron microscopy (TEM, FEI Tecnai F-20 microscopy) in the STEM mode.

## 3. Results and discussion

Fig. 1 illustrates the XRD pattern of nanowires, indicating the presence of crystalline würtzite structure for ZnO (JCPDS no. 79-0208) and tetragonal cassiterite structure for $SnO_2$ (JCPDS no. 77-0449). In addition, the diffraction lines resulting from the substrate are also observed. Additionally, some peaks of ternary compound of face centered cubic spinel $Zn_2SnO_4$ (JCPDS no. 24-1470) are also detected. This result indicates that a part of $SnO_2$ and ZnO react to form $Zn_2SnO_4$. The presence of sharp and strong X-ray diffraction peaks

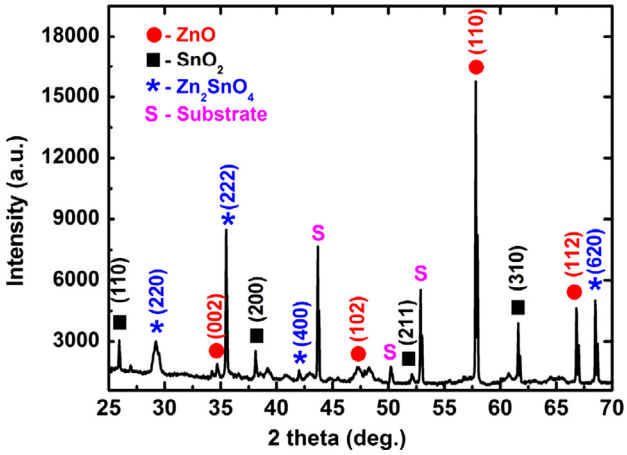


Fig. 1. XRD patterns of ZnO/$SnO_2$ mixed nanowires.

suggests that the ZnO/$SnO_2$ mixed nanowires are well crystallized.

FESEM micrographs of the samples prepared at 900 °C for 2 h are shown in Fig. 2. Two control experiments were performed to find the effect of Au layer and activated carbon on nanowire growth. In Fig. 2(a), it is seen that no nanowires are observed in the absence of Au on alumina substrate with the presence of activated carbon. Similarly, no nanowires are present on Au/alumina substrate in the absence of activated carbon as it can be seen in Fig. 2(b). Here, spheroidal shaped Au particles are seen that are formed by dewetting of the Au layer. But, in the presence of both carbon and Au, uniform and well distributed nanowires can be seen on Au/alumina substrate (Fig. 2(c)). The diameter of the nanowires is in the range of 15–80 nm with a length of 16–50 μm. The inset of Fig. 2(c) shows the enlarged image of the tip of a nanowire. The presence of the Au cap at the tip of the nanowire is a strong evidence that the growth of nanowires is by the vapor–liquid–solid (VLS) assisted mechanism [27]. It is believed that at 900 °C, the activated carbon dissociates ZnO and $SnO_2$ powders into Zn and Sn vapors, which condense on the Au/alumina substrate at lower temperature. The Sn and Zn metal vapors react with Au layer and form an alloy droplet on the alumina substrate. This alloy droplet becomes super saturated after receiving more metal vapors that initiates the nanowire growth. Therefore, the presence of activated carbon and Au are essential for the growth of nanowires, where the activated carbon acts as a reducing agent producing the metal vapors and the Au acts as a catalyst to grow the nanowires.

Different types of nanostructures are observed under FESEM at different locations on the Au/alumina substrate, which are illustrated in Fig. 3(a) and (b). Fig. 3(a) shows a comb-like branch structure of ZnO/$SnO_2$ nanowires. In this structure, the diameter of the backbone nanowire is 80 nm and the branched nanowires show a uniform diameter of 30 nm (Inset of Fig. 3(a)). Fig. 3(b) illustrates the morphology of ZnO/$SnO_2$ hierarchical nanostructure. More importantly, the secondary branches from backbone nanowires are noteworthy (Inset of Fig. 3(b)). The end of these secondary branches has Au tip which indicates that VLS mechanism is operative

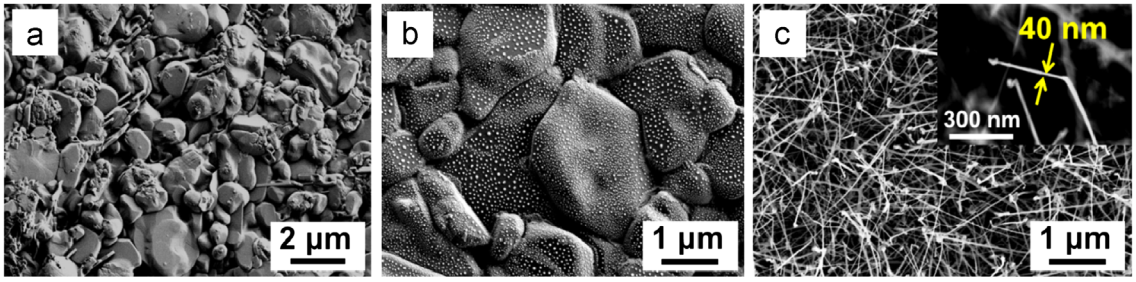


Fig. 2. FESEM images of the nanostructures of samples prepared at 900 °C for 2 h grown on (a) alumina substrate in the presence of activated carbon, (b) Au/alumina substrate in the absence of activated carbon and (c) Au/alumina substrate in the presence of activated carbon.

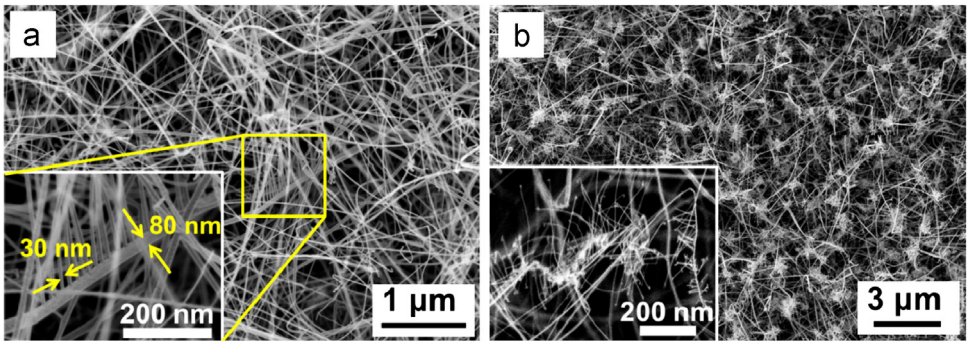


Fig. 3. FESEM micrographs of $ZnO/SnO_2$ mixed nanowires: (a) comb-like and (b) hierarchical nanostructures.

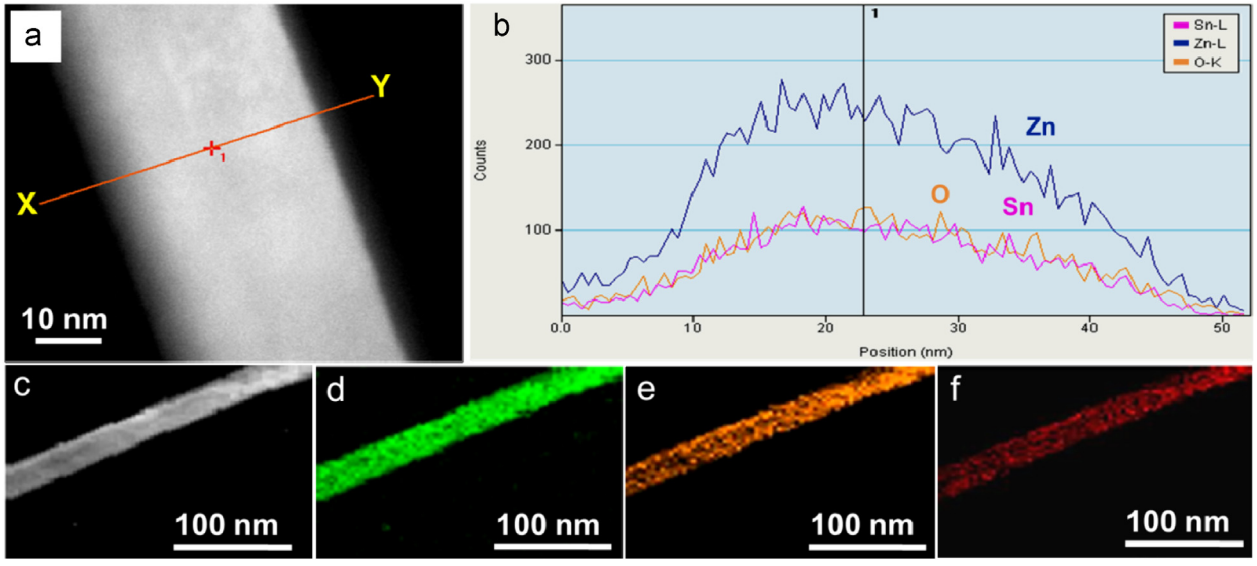


Fig. 4. (a) Magnified STEM image of $ZnO/SnO_2$ nanowire, (b) cross-sectional compositional line profiles of Zn, Sn and O, (c) EDX elemental mapping of $ZnO/SnO_2$ nanowire demonstrating the spatial distribution of (d) Zn, (e) Sn, and (f) O.

here. Au plays an important role of catalysts to grow both the branch and hierarchical nanowires. This kind of hierarchical nanostructures have been reported by various fabrication methods [20,22]. In our study, hierarchical nanostructures consist of trunk and branches, which are composed of mixed $ZnO/SnO_2$ material. However, a controlled synthesis of these kinds of nanostructures is still a challenge. It has been suggested that the backbone nanowire grew quickly with the Au catalyst particle at the tip, while smaller alloy droplets would be formed on the backbone nanowire surface which leads to the hierarchical nanowires in different location [28]. The growth of hierarchical nanowires is triggered, when the critical value of temperature and vapor supersaturation ratio is achieved. In our case, we cannot clearly state which factor mostly influences the hierarchical nanowires. Further study is underway to clarify this issue.

Fig. 4(a) and (b) shows concentration line profiles of Zn, Sn and O across a nanowire. The profile suggests that both Sn and

Zn are homogeneously distributed within the nanowire and Zn is richer than Sn. Additionally, Fig. 4(d)–(f) demonstrates uniform spatial distribution of Zn, Sn, and O in EDX elemental mapping shown in Fig. 4(c). This result clearly indicates that ZnO and $SnO_2$ are mixed throughout the nanowires that are synthesized by the single-step carbothermal reduction method. This is very different than what is reported in literature, where they grow sequentially on top of each other. This clearly represents a simple process to grow mixed nanowires with homogeneous composition with potential applications in chemical sensing and other devices.

## 4. Conclusions

In summary, this study verifies that a large number of ZnO/$SnO_2$ mixed nanowires per unit area can be grown on Au/alumina substrate by employing a single-step carbothermal reduction method. The role of the activated carbon and Au are systematically studied. According to TEM results, mixed ZnO/$SnO_2$ phases are confirmed to be uniformly distributed throughout the nanowire. The catalyst assisted growth of nanowire on alumina substrate constitutes to be a promising method to grow nanowires over large area. The unique morphology and homogeneous composition of ZnO/$SnO_2$ mixed nanowires may lead to their potential applications.

## Acknowledgments

The authors acknowledge the financial support of High Impact Research grant (HIR no. M.C/625/1/HIR/040) and UMRG grant (UMRG no. RP021-2012D) from the University of Malaya. Ms. T. Tharsika acknowledges the Bright Spark Unit, University of Malaya for a bright spark scholarship and thanks to Mr. M.M. Arafat for his help in proof reading the manuscript.

## References

[1] Z.L. Wang, Zinc oxide nanostructures: growth, properties and applications, Journal of Physics: Condensed Matter 16 (2004) R829–R858.
[2] C.M. Lieber, One-dimensional nanostructures: chemistry, physics and applications, Solid State Communications 107 (1998) 607–616.
[3] A. Kolmakov, M. Moskovits, Chemical sensing and catalysis by one-dimensionalmetal-oxide nanostructures, Annual Review of Materials Research 34 (2004) 151–180.
[4] F. Patolsky, G. Zheng, C.M. Lieber, Nanowire sensors for medicine and the life sciences, Nanomedicine 1 (2006) 51–65.
[5] T. Zhai, X. Fang, M. Liao, X. Xu, H. Zeng, B. Yoshio, D. Golberg, A comprehensive review of one-dimensional metal-oxide nanostructure photodetectors, Sensors 9 (2009) 6504–6529.
[6] J. Chen, L.-n. Xu, W.-y. Li, X.-l. Gou, α-$Fe_2O_3$ nanotubes in gas sensor and lithium-ion battery applications, Advanced Materials 17 (2005) 582–586.
[7] S. Sen, P. Kanitkar, A. Sharma, K.P. Muthe, A. Rath, S.K. Deshpande, M. Kaur, R.C. Aiyer, S.K. Gupta, J.V. Yakhmi, Growth of $SnO_2$/$W_{18}O_{49}$ nanowire hierarchical heterostructure and their application as chemical sensor, Sensors and Actuators B: Chemical 147 (2010) 453–460.
[8] I.S. Hwang, S.J. Kim, J.K. Choi, J. Choi, H. Ji, G.T. Kim, G. Cao, J.H. Lee, Synthesis and gas sensing characteristics of highly crystalline ZnO–$SnO_2$ core–shell nanowires, Sensors and Actuators B: Chemical 148 (2010) 595–600.
[9] J.A. Park, J. Moon, S.J. Lee, S.H. Kim, H.Y. Chu, T. Zyung, $SnO_2$–ZnO hybrid nanofibers-based highly sensitive nitrogen dioxides sensor, Sensors and Actuators B: Chemical 145 (2010) 592–595.
[10] X. Song, D. Zhang, M. Fan, A novel toluene sensor based on ZnO–$SnO_2$ nanofiber web, Applied Surface Science 255 (2009) 7343–7347.
[11] N.D. Khoang, D.D. Trung, N. Van Duy, N.D. Hoa, N. Van Hieu, Design of $SnO_2$/ZnO hierarchical nanostructures for enhanced ethanol gas-sensing performance, Sensors and Actuators B: Chemical 174 (2012) 594–601.
[12] Y.J. Chen, G. Xiao, T.S. Wang, F. Zhang, Y. Ma, P. Gao, C.L. Zhu, E. Zhang, Z. Xu, Q. Li, Synthesis and enhanced gas sensing properties of crystalline $CeO_2$/$TiO_2$ core/shell nanorods, Sensors and Actuators B: Chemical 156 (2011) 867–874.
[13] J.Y. Park, S.W. Choi, J.W. Lee, C. Lee, S.S. Kim, Synthesis and gas sensing properties of $TiO_2$–ZnO core-shell nanofibers, Journal of the American Ceramic Society 92 (2009) 2551–2554.
[14] Y.J. Chen, C.L. Zhu, L.J. Wang, P. Gao, M.S. Cao, X.L. Shi, Synthesis and enhanced ethanol sensing characteristics of α-$Fe_2O_3$/$SnO_2$ core–shell nanorods, Nanotechnology 20 (2009) 045502.
[15] C. Zhu, Y. Chen, R. Wang, L. Wang, M. Cao, X. Shi, Synthesis and enhanced ethanol sensing properties of α-$Fe_2O_3$/ZnO heteronanostructures, Sensors and Actuators B: Chemical 140 (2009) 185–189.
[16] I.Y.Y. Bu, Novel all solution processed heterojunction using p-type cupric oxide and n-type zinc oxide nanowires for solar cell applications, Ceramics International 39 (2013) 8073–8078.
[17] N. Talebian, F. Jafarinezhad, Morphology-controlled synthesis of $SnO_2$ nanostructures using hydrothermal method and their photocatalytic applications, Ceramics International 39 (2013) 8311–8317.
[18] Y.T. Lim, J.Y. Son, J.S. Rhee, Vertical ZnO nanorod array as an effective hydrogen gas sensor, Ceramics International 39 (2013) 887–890.
[19] E.M. El-Maghraby, A. Qurashi, T. Yamazaki, Synthesis of $SnO_2$ nanowires their structural and $H_2$ gas sensing properties, Ceramics International 39 (2013) 8475–8480.
[20] C. Cheng, B. Liu, H. Yang, W. Zhou, L. Sun, R. Chen, S.F. Yu, J. Zhang, H. Gong, H. Sun, Hierarchical assembly of ZnO nanostructures on $SnO_2$ backbone nanowires: low-temperature hydrothermal preparation and optical properties, ACS Nano 3 (2009) 3069–3076.
[21] Y. Zhang, K. Yu, S. Ouyang, Z. Zhu, Patterned growth and field emission of ZnO nanowires, Materials Letters 60 (2006) 522–526.
[22] C. Lan, J. Gong, Y. Su, K. Li, S. Yang, Synthesis and photoluminescence properties of $SnO_2$/ZnO hierarchical nanostructures, Physica E: Low-dimensional Systems and Nanostructures 44 (2012) 791–796.
[23] P. Yang, H. Yan, S. Mao, R. Russo, J. Johnson, R. Saykally, N. Morris, J. Pham, R. He, H.J. Choi, Controlled growth of ZnO nanowires and their optical properties, Advanced Functional Materials 12 (2002) 323.
[24] Y.F. Tu, Q.M. Fu, J.P. Sang, Z.J. Tan, X.W. Zou, Effects of annealing temperature on the properties of ZnO/$SnO_2$ core/shell nanorod arrays, Materials Letters (2012) 80–83.
[25] G. Shen, Fabrication and characterization of metal oxide nanowire sensors, Recent Patents on Nanotechnology 2 (2008) 160–168.
[26] A. Johari, V. Rana, M. Chander Bhatnagar, Synthesis, characterization and ethanol sensing properties of tin oxide nanostructures, Nanomaterials and Nanotechnology 1 (2011) 49–54.
[27] B. Wang, Y. Yang, C. Wang, G. Yang, Growth and photoluminescence of $SnO_2$ nanostructures synthesized by Au–Ag alloying catalyst assisted carbothermal evaporation, Chemical Physics Letters 407 (2005) 347–353.
[28] Y. Zhang, R. Li, X. Zhou, M. Cai, X. Sun, Hierarchical $Al_2O_3$ nanobelts and nanowires: morphology control and growth mechanism, Crystal Growth and Design 9 (2009) 4230–4234.